Journal of Photochemistry and Photobiology A: Chemistry 214 (2010) 10–15

Contents lists available at ScienceDirect

Journal of Photochemistry and Photobiology A: Chemistry

journal homepage: www.elsevier.com/locate/jphotochem

Excited-state levels and relaxation processes of chromone and 6-fluorochromone vapors

Takao Itoh *

Graduate School of Integrated Arts and Science, Hiroshima University, 1-7-1 Kagamiyama, Higashi-Hiroshima City 739-8521, Japan

ARTICLE INFO

Article history:
Received 1 March 2010
Received in revised form 4 May 2010
Accepted 31 May 2010
Available online 8 June 2010

Keywords:
Chromone
Vapor phase
Phosphorescence
Temperature dependence
Energy levels

ABSTRACT

Emission and excitation spectra of chromone and 6-fluorochromone have been measured in the vapor phase at different temperatures and pressures along with the absorption spectra. The emission is shown to consist of the $^3(\mathrm{n}, \pi^*)$ phosphorescence accompanied by weak $S_1(\mathrm{n}, \pi^*)$ delayed fluorescence. It is inferred from the temperature dependence of the phosphorescence intensity that the $^3(\mathrm{n}, \pi^*)$ state is located at energies below the $^3(\pi, \pi^*)$ state for chromone and 6-fluorochromone vapors. The relaxation processes in the vapor phase are discussed based on the pressure and excitation energy dependence of the relative phosphorescence yields. The data include the vibrational analyses of the emission spectra based on the results of the DFT calculations at the B3LYP/6-311 + G(p, d) level.

© 2010 Elsevier B.V. All rights reserved.

1. Introduction

Photochemical behavior of chromone has been investigated intensively, and the nature of the lowest excited state T_1, $^3(\mathrm{n}, \pi^*)$ or $^3(\pi, \pi^*)$, has been discussed based on the photoproducts [1–7]. It is known that normally the type of photoproduct of the carbonyl compounds differs significantly depending on the nature of the T_1 state. The T_1 state of chromone has been investigated also spectroscopically [8–12]. It was reported that the T_1 state of chromone is of $^3(\pi, \pi^*)$ type in polar solvents such as ethanol, but is of $^3(\mathrm{n}, \pi^*)$ type in non-polar solvents such as 3-methypentane at 77 K [7]. However, it was also suggested based on the high-resolution experiments at He temperature that the T_1 state of chromone is of $^3(\pi, \pi^*)$ type in non-polar solvents such as 3-methylpentane and methylcyclohexane [9]. In any case, the lowest $^3(\pi, \pi^*)$ and $^3(\mathrm{n}, \pi^*)$ states of chromone are considered to be located very closely to each other, but the ordering of these two triplet states seems to be still in controversy. It is, therefore, of importance to determine the state ordering as well as the accurate location of the triplet states of chromone in the vapor phase where the molecules suffer no interaction from the environment. Nevertheless, at present no information is available for the emission and absorption spectral data of chromone in the vapor phase. This is presumably due to the low emission quantum yield and low vapor pressure as well as to the chemical instability of chromone vapor with respect to photon irradiation.

In general, the phosphorescence spectral data of organic molecules in the vapor phase are scarce. In addition, only some of the phosphorescent molecules show detectable sharp emission bands in the vapor phase. Nevertheless, without the acquirement of the emission spectra showing sharp bands, it is almost impossible to investigate the interaction between the electronic and vibrational states. In order to obtain vibrationally resolved spectra, therefore, it is of importance to access the molecules which show the sharp phosphorescence bands in the vapor phase.

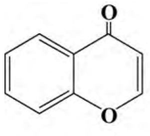

Chromone

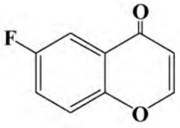

6-Fluorochromone

In the present study, vibrationally resolved emission spectra have been measured for chromone and 6-fluorochromone vapors at different temperatures. The latter molecule is expected to possess the excited-state electronic structure similar to that of chromone. It is shown that chromone and 6-fluorochromone exhibit comparatively sharp phosphorescence bands in the vapor phase. The emission is shown to consist of the $^3(\mathrm{n}, \pi^*)$ phosphorescence accompanied by the weak $S_1(\mathrm{n}, \pi^*)$ delayed fluorescence. The locations of the $T_1(\mathrm{n}, \pi^*)$ and $S_1(\mathrm{n}, \pi^*)$ origins have been determined in the vapor phase. The vibronic bands in the emission spectra were assigned based on the results of the DFT calculations at the B3LYP/6-311 + G(p, d) level. It is inferred from the temperature dependence of the phosphorescence intensity that the $^3(\mathrm{n}, \pi^*)$ state is located at energies below the $^3(\pi, \pi^*)$ state for chromone and

---

* Tel.: +81 824 24 6535, fax: +81 824 24 0757.
E-mail address: titoh@hiroshima-u.ac.jp.

1010-6030/$ – see front matter © 2010 Elsevier B.V. All rights reserved.
doi:10.1016/j.jphotochem.2010.05.022

6-fluorochromone vapors. The relative phosphorescence quantum yields are found to decrease with increasing excitation energy and with decreasing pressure. The relaxation processes in the vapor phase are discussed based on the pressure and excitation energy dependence of the relative phosphorescence yield.

2. Experimental and computational methods

Chromone obtained from Tokyo Chemical Industry, Japan, and 6-fluorochromone obtained from Aldrich were purified by means of repeated recrystallization from hexane. Absence of any impurity emission in glassy matrix at 77 K and verification that the excitation spectra in the vapor phase agreed well with the corresponding absorption spectra suggest that the purified samples are sufficiently pure for the experiment. Perfluorohexane obtained from Aldrich, USA, was used as a buffer gas. The sample was carefully degassed by repeating freeze–thaw cycles in an all-glass made vacuum system equipped with a diffusion pump: a small amount of the sample crystal was put into the cell and then the buffer gas was introduced to the sample cell after degassing of the crystal as well as the buffer gas. The details of the sample preparation method are described in a foregoing paper [13]. The samples were found to be unstable with respect to photon irradiation and to degrade during long-time measurements. Thus, all the measurements were carried out only once for each fresh sample just after the preparation. It took about 100 min for measuring each emission spectrum and about 60 min for measuring each excitation spectrum. It was confirmed that no appreciable change was detected for the spectral intensities before and after the measurement. In most of the spectral measurements, square 10-mm path length quartz cells were used and the temperature of the cell was controlled by a thermostated cell holder. A cylindrical 100-mm path length quartz cell was used for measuring weak absorption spectra.

Absorption spectra were measured with a Shimadzu UV-2550 spectrophotometer and the emission and excitation spectra were measured with a Spex Fluorolog-3 (Model 21-SS) spectrophotometer. Two reflection mirrors were placed beside the sample cell holder to intensify the emission signals [14]. The slit width used for measuring the absorption, emission and excitation spectra is kept 2.0 Å. The wavelength calibration was carried out using a Melles Griot He–Ne green laser. Emission spectra were corrected for the spectral sensitivity of the detection system by comparing the measured spectrum with the real spectrum using quinine in sulfuric acid as the standard. Excitation spectra were corrected for the spectral intensity distribution of the exciting light with an aqueous solution of rhodamine B as a quantum counter.

Quantum chemical calculations were carried out with the density-functional theory (DFT) using GAUSSIAN 03 program [15]. Optimized geometries, total energies and harmonic wavenumbers in the ground state, ν_{harm}, were obtained by the DFT calculations at the B3LYP/6-311 + G(d, p) level. The calculated wavenumbers, ν_{calc}, in the ground state were scaled using the relation, $\nu_{\mathrm{calc}} = \nu_{\mathrm{harm}} \times (1.0087 - 0.0000163 \times \nu_{\mathrm{harm}})$, to reproduce the anharmonicity of observed vibrations, where ν_{harm} denotes the harmonic frequency obtained by the DFT calculation [16].

3. Results and discussion

3.1. Emission spectra and the electronic-state ordering

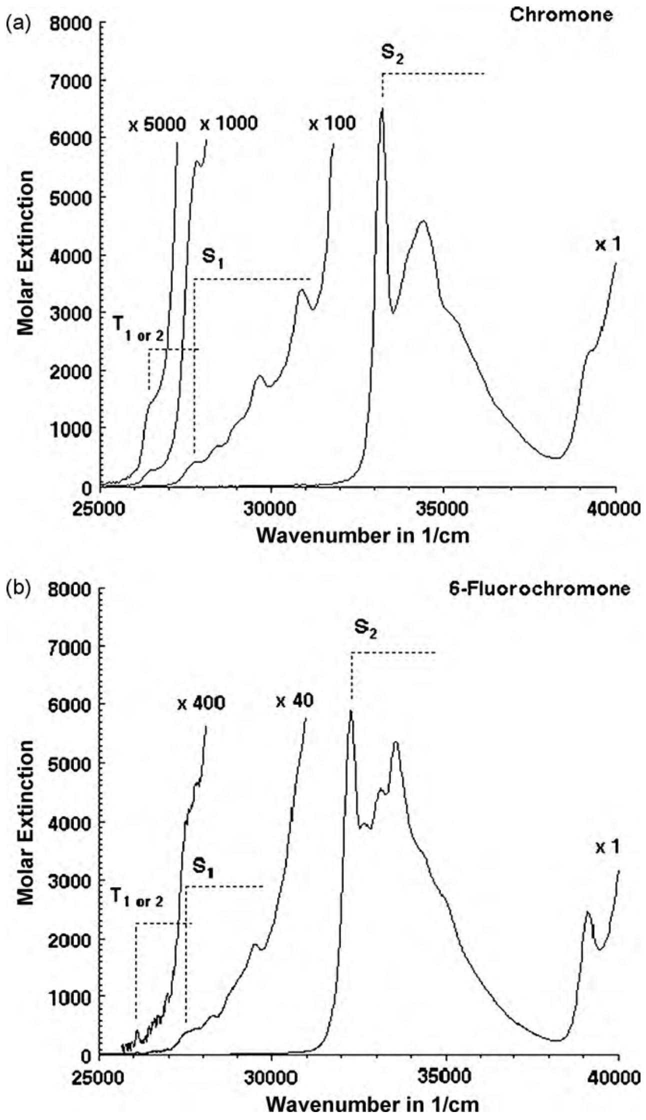

Fig. 1. Absorption spectra of chromone (a) and 6-fluorochromone (b) in hexane at room temperature. The concentrations of chromone and 6-fluorochromone in hexane are below 10^{-3} mol/l.

Absorption spectra of chromone and 6-fluorochromone in hexane at room temperature are shown in Fig. 1a and b, respectively. In hexane, the absorption spectrum of chromone consists of the weak $S_0 \rightarrow {}^3(n, \pi^*)$, $S_0 \rightarrow S_1(n, \pi^*)$ and comparatively strong $S_0 \rightarrow S_2(\pi, \pi^*)$ bands with the origins seen at 26,300, 27,700 and 33,100 cm^{-1}, respectively, and with the molar extinction coefficients of the origin bands of 0.3, 5.0 and 6450. The absorption spectrum of 6-fluorochromone resembles that of chromone and the origin bands of the $^3(n, \pi^*)$, $S_1(n, \pi^*)$ and $S_2(\pi, \pi^*)$ states are seen at 26,100, 27,550 and 32,280 cm^{-1}, respectively, with the molar extinction coefficients of the origin bands of 0.4, 10.0 and 5900. The absorption spectra in solution provide the approximate locations of the excited triplet and singlet (n, π*) states, but may not provide the information on the locations of the triplet (π, π*) states.

The emission spectra of chromone and 6-fluorochromone vapors in the presence of 250 Torr perfluorohexane at different temperatures are shown in Fig. 2a and b, respectively. In the present experiment, a buffer gas was added to the samples, since the emission of the samples is weak without buffer gas and since addition of buffer gas induces the efficient collisional relaxation to the lower-lying excited states. As will be shown later in detail, the excitation spectra of the observed emission agree well with the absorption spectra. The emission of chromone and 6-fluorochromone vapors consists of the weak fluorescence from $S_1(n, \pi^*)$ and phosphorescence from $^3(n, \pi^*)$, showing a prominent progression in the C=O stretching vibration in the phosphorescence spectra. The

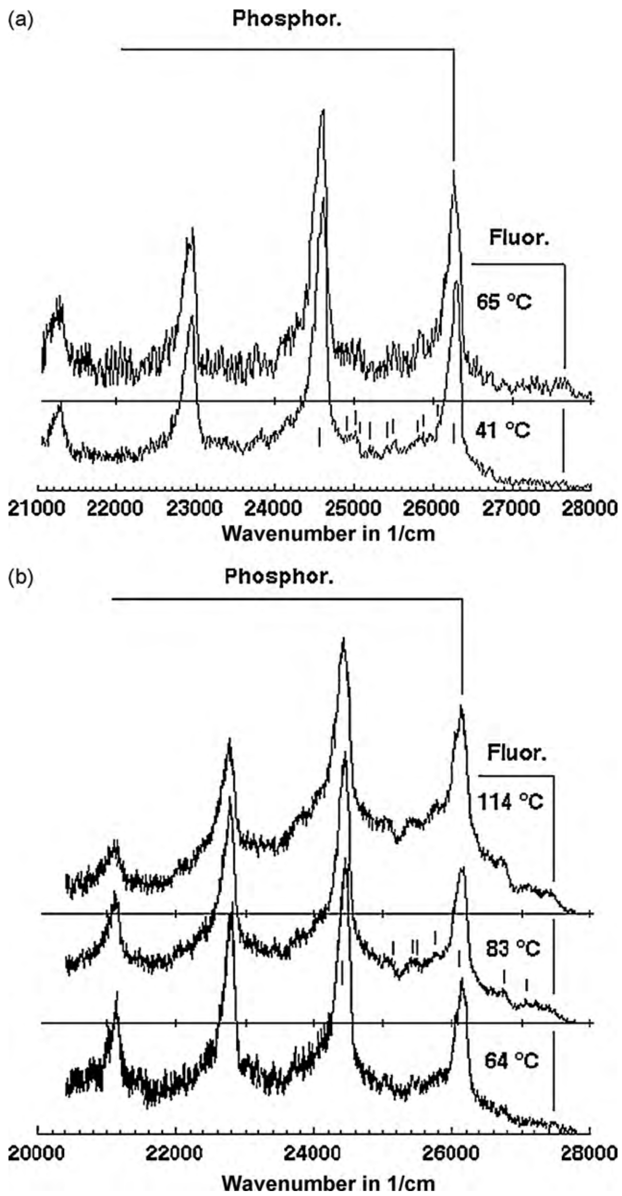

Fig. 2. Emission spectra of chromone (a) and 6-fluorochromone (b) vapors in the presence of 250 Torr perfluorohexane at different temperatures. The pressure of chromone changes from 0.15 to 0.9 Torr by varying the temperature from 40 to 70 °C and that of 6-fluorochromone changes from 0.3 to 4 Torr by varying the temperature from 60 to 110 °C. Sticks indicate the observed band locations. All the spectra are normalized to a common magnitude.

Table 1
Frequencies (ν) and assignments of the bands observed in the emission spectrum of chromone vapor.

ν (cm^{-1})[a]	$\Delta\nu$ (cm^{-1})[b]	Assignment[c]	Calculated $\Delta\nu$ (cm^{-1})[d]
27,645	0	S_1(n, π^*) origin	
26,295	0	T_1(n, π^*) origin	
26,055	240	op. ring	242.1
25,830	465	op. ring	465.7
25,765	530	ip. ring	534.4
25,485	810	ip. ring	810.2
25,410	885	op. C–H bend	881.9
25,210	1085	ip. ring	1089.5
25,055	1240	ip. C–H bend	1241.4
25,030	1265	ip. C–H bend	1263.2
24,945	1350	ip. ring	1348.3
24,605	1690	C=O stretch.	1685.2
24,145	1250	1690 + 465	
24,060	2225	1690 + 530	
23,725	2570	1690 + 885	
23,360	2935	1690 + 1240	
23,335	2960	1690 + 1265	
23,255	3040	1690 + 1350	
22,930	3365	1690 × 2	
22,460	3835	1690 × 2 + 465	
22,120	4175	1690 × 2 + 810	
21,565	4720	1690 × 2 + 1350	
21,260	5035	1690 × 3	

[a] Accuracy of ± 5 cm^{-1}.
[b] Separation from the origin.
[c] ip. and op. represent in-plane and out-of-plane modes, respectively.
[d] Obtained with the DFT calculation at the B3LYP/6-311 + G(d, p) level with scaling by the relation, $\nu_{calc} = \nu_{harm} \times (1.0087 - 0.0000163 \times \nu_{harm})$.

phosphorescence and fluorescence origins of chromone vapor are observed at 26,295 and 27,645 cm^{-1}, respectively, and those of 6-fluorochromone vapor are observed at 26,155 and 27,435 cm^{-1}, respectively. The locations of the phosphorescence and fluorescence origins in the vapor phase agree with those of the $S_0 \rightarrow {}^3$(n, π^*) and $S_0 \rightarrow S_1$(n, π^*) absorption origins in hexane, respectively.

The observed emission spectra exhibit characteristic temperature dependence. That is, the S_1 fluorescence intensity relative to the phosphorescence intensity increases with increasing temperature. The feature of the fluorescence is the characteristic of the thermally activated delayed fluorescence from S_1, which is in thermodynamic equilibrium with the phosphorescent state [17]. Thus, the quantum yield ratio of the emission from the upper state (S_1) to that from the lower triplet state, Φ_F/Φ_P, is given approximately by $\Phi_F/\Phi_P = (k_F/k_P) \times \exp[-\Delta E_{S-T}/kT]$, where ΔE_{S-T} is the $S_1 - T$ energy separation, k_F and k_P are, respectively, the radiative rate constants of the S_1 and T states and k is the Boltzmann constant. We have used the integrated intensities of the fluorescence and phosphorescence origins subtracted by the background intensities, I_F and I_P, instead of Φ_F and Φ_P, respectively. (As for the phosphorescence, the intensities in the origin peak ranging from 26,000 to 26,500 cm^{-1} and 25,800 to 26,200 cm^{-1} were integrated, respectively, for chromone and 6-fluorochromone, and as for the fluorescence, the intensities ranging from 27,000 to 27,800 cm^{-1} were integrated.) The values for ΔE_{S-T} obtained from the logarithmic plots of I_F/I_P versus reciprocal of the absolute temperature ($1/T$) are 1300 ± 200 and 1200 ± 200 cm^{-1}, respectively, for chromone and 6-fluorochromone vapors. The ΔE_{S-T} values thus estimated agree with the spectroscopically estimated singlet–triplet (n, π^*) energy separations of 1350 and 1280 cm^{-1}, respectively, for chromone and 6-fluorochromone vapors. The locations and assignments of the bands observed in the emission spectra of chromone and 6-fluorochromone vapors are summarized in Tables 1 and 2, respectively. Most of the vibrational bands appearing in the emission spectra are interpreted in terms of the C=O stretching mode and the modes combined with it.

We have observed the phosphorescence from the ^{3}(n, π^*) state for chromone and 6-fluorochromone vapors. However, the fact that the ^{3}(n, π^*) phosphorescence was observed does not necessarily indicate that the ^{3}(n, π^*) state is the lowest excited triplet state. Even though the ^{3}(π, π^*) state is located at energies below the ^{3}(n, π^*) state, the ^{3}(n, π^*) phosphorescence is often observed due to the thermal activation of the ^{3}(π, π^*) state, when the two triplet states are located closely to each other (see Fig. 3) [13]. It was shown in a previous paper that the ^{3}(n, π^*) phosphorescence quantum yield increases with increasing temperature for the molecules where the ^{3}(π, π^*) state is located at energies below the ^{3}(n, π^*) state [13]. On the other hand, for the molecules where the ^{3}(n, π^*) state is located at energies below the ^{3}(π, π^*) state, the ^{3}(n, π^*) phosphorescence quantum yield normally decreases with increasing temperature [13]. In order to confirm the state ordering of the two triplet states, the temperature dependence of the relative phosphorescence yield

Table 2
Frequencies (ν) and assignments of the bands observed in the emission spectrum of 6-fluorochromone vapor.

ν (cm^{-1})[a]	$\Delta\nu$ (cm^{-1})[a]	Assignment[a]	Calculated $\Delta\nu$ (cm^{-1})[a]
27,435	0	S_1(n, π*) origin	
27,100	335	op. ring	338.8
26,750	685	op. ring	680.4
26,155	0	T_1(n, π*) origin	
25,760	395	ip. C–F bend	398.2
25,445	710	ip. ring	711.0
25,400	755	op. ring	756.2
25,120	1035	ip. C–H bend	1034.8
24,450	1705	ip. C=O stretch	1686.2
24,270	1885	1705 + 180 (op. ring)	182.7 + 1686.2
24,055	2100	1705 + 395	
23,740	2415	1705 + 710	
23,415	2750	1705 + 1035	
22,780	3375	1705 × 2	
22,385	3770	1705 × 2 + 395	
21,745	4410	1705 × 2 + 1035	
21,140	5015	1705 × 3	

[a] Same as in Table 1.

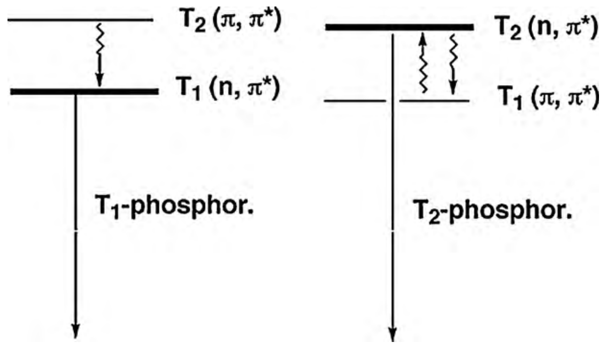

Fig. 3. Scheme showing the phosphorescence process from the closely lying triplet (n, π*) and (π, π*) states in the vapor phase at temperatures near room temperature.

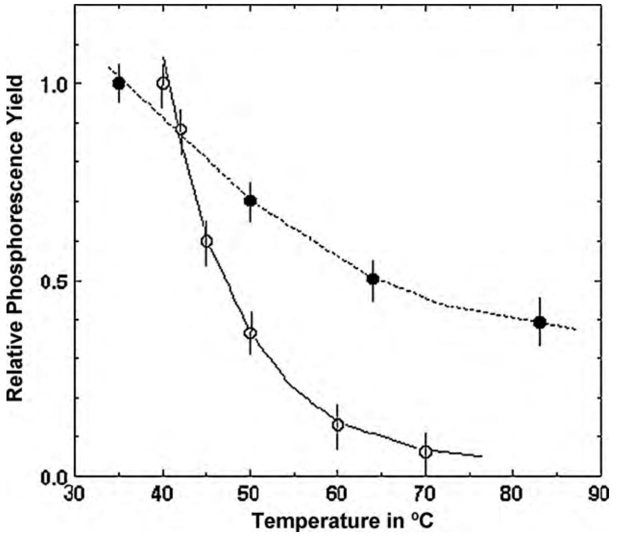

Fig. 4. The relative phosphorescence yields plotted against the temperature for chromone (open circles) and 6-fluorochromone (closed circles) vapors in the presence of 250 Torr perfluorohexane.

has been investigated. As one can see in Fig. 4, the relative phosphorescence yield decreases significantly with increasing temperature for chromone and 6-fluorochromone vapors. These observations suggest that the ^{3}(n, π*) state is located at energies below the ^{3}(π, π*) state for the two molecules in the vapor phase.

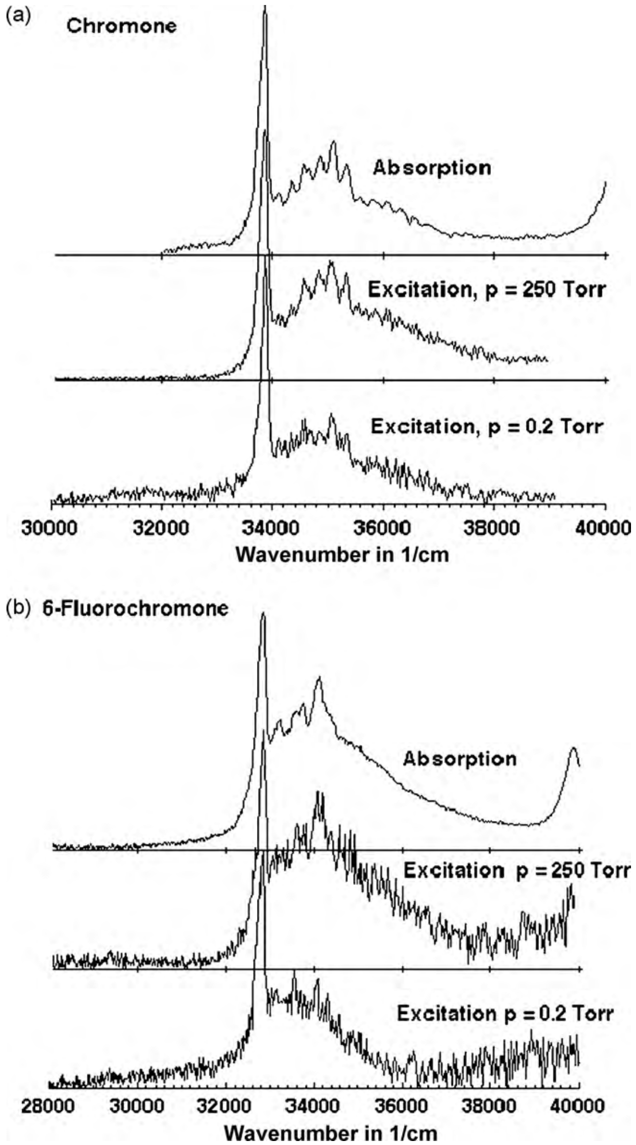

Fig. 5. Absorption and excitation spectra of chromone (a) and 6-fluorochromone (b) vapors: the excitation spectra are shown for the samples with (p = 250 Torr) and without perfluorohexane (p = 0.2 Torr) as added buffer gas. All the spectra are normalized to a common magnitude.

The state ordering between the ^{3}(n, π*) and ^{3}(π, π*) states of chromone and 6-fluorochromone may be correlated also with the location of the S_2(π, π*) states. In hexane at room temperature, the S_2(π, π*) origin of chromone is located at 33,100 cm^{-1}, but in the vapor phase it is located at 33,880 cm^{-1}. Thus, it is not unreasonable to consider that the ^{3}(π, π*) state shows the corresponding blue shift on going from hexane solution to the vapor phase, thereby ^{3}(n, π*) is located at energies below ^{3}(π, π*) in the vapor phase.

3.2. Relaxation processes of the excited state

Fig. 5a and b shows the absorption and excitation spectra of chromone and 6-fluorochromone vapors in the $S_0 \rightarrow S_2$(π, π*) region, respectively. We could not measure the absorption and excitation spectra in the $S_0 \rightarrow S_1$(n, π*) region because of the low vapor pressure and low molar extinction coefficient. In the presence of 250 Torr perfluorohexane, the corrected excitation spectrum agrees well with the absorption spectrum, but at low pressure without the buffer gas the intensities of the excitation spectrum

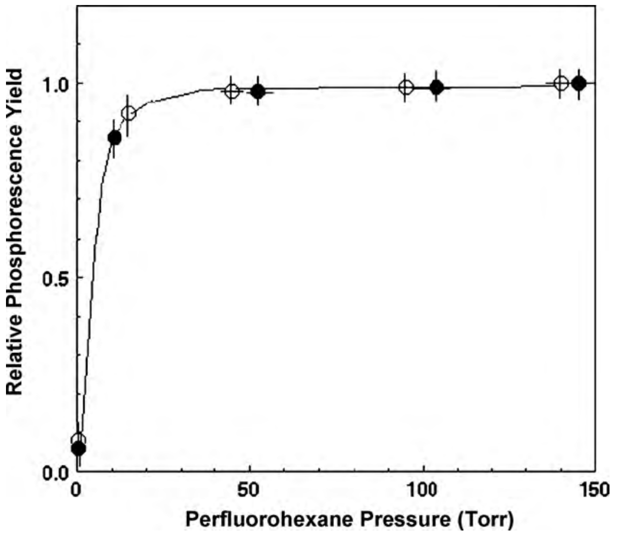

Fig. 6. The relative phosphorescence quantum yield Φ_P of chromone (open circles) and 6-fluorochromone (closed circles) vapors plotted against the pressure of added buffer gas at 40 °C.

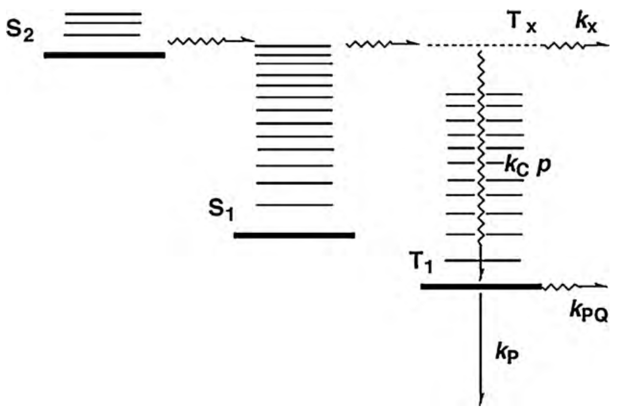

Fig. 7. Kinetic scheme explaining pressure dependence of the relative phosphorescence quantum yield of chromone vapors.

at higher wavenumbers are too low as compared with those of the absorption spectrum. This observation indicates that at low pressure the phosphorescence quantum yield decreases with increasing excitation energy.

Fig. 6 shows the relative phosphorescence quantum yield Φ_P of chromone and 6-fluorochromone vapors plotted against the pressure of added perfluorohexane, p, where the Φ_P values are obtained by the excitation into the $S_2(\pi, \pi^*)$ origin and by dividing the integrated intensity by the optical density of the sample at each temperature. As p is reduced, Φ_P appears to approach a zero value. The excitation spectrum at low pressure indicates that the decrease of Φ_P caused by lowering the pressure becomes more pronounced as the excitation energy is increased.

The pressure dependence of the phosphorescence quantum yield of chromone vapors can be explained in terms of a kinetic scheme shown in Fig. 7, where T_x represents a state from which chromone molecule takes place the decomposition or nonradiative transition to the ground state. The molecules excited into the S_2 state will be converted to the S_1 molecule through the fast internal conversion. The T_x molecule formed as the result of the intersystem crossing from S_1 will be deactivated to the lower vibrational levels of T_1 through the collision with the rate $k_C \times p$, from which the molecule shows the phosphorescence. The conversion to the T_x state is followed by the decomposition or nonradiative transition to the ground state with the rate constant k_x, but with increasing pressure collisional deactivation to the lower vibrational levels of T_1 competes with the decomposition. The kinetic scheme accounts for the observation that the relative phosphorescence quantum yield, Φ_P, increases with increasing pressure.

In terms of the scheme shown in Fig. 7, Φ_P is given by

$$\Phi_P = \Phi_{isc} \times \frac{k_C \times p}{k_C \times p + k_x} \times \left[\frac{k_P}{k_P + k_{PQ}} \right], \tag{1}$$

where Φ_{isc} is the quantum yields of the overall conversion from S_2 to T_x, and k_P and k_{PQ} are the radiative and nonradiative rate constants of the T_1 state, respectively. By fitting the experimental data given in Fig. 6 to Eq. (1), the values for k_x/k_C are evaluated to be 1.2 and 1.6 Torr, respectively, for chromone and 6-fluorochromone. In terms of the kinetic model, the lifetime of the T_x state is given by $1/(k_x + k_C \times p)$. If k_C is assumed to be equal to the bimolecular rate constant for collision ($\sim 10^7$ Torr^{-1} s^{-1}), then the k_x value can be obtained from the k_x/k_C value already determined. The lifetimes of the T_x state at zero pressure ($1/k_x$) are obtained to be 8.3×10^{-8} and 6.3×10^{-8} s, respectively, for chromone and 6-fluorochromone vapors. Since we have not observed the strong prompt fluorescence neither from the S_1 nor S_2 state, the T_x state cannot be the S_2 or S_1 state. The state conceivable for T_x is, therefore, one of the following: the high vibrational levels in the T_1 state, a higher triplet state T_j with $j > 1$, or a reaction intermediate which cannot be identified as any of the excited states of chromone molecules.

4. Conclusions

Emission of chromone and 6-fluorochromone is shown to consist of the $T_1(n, \pi^*)$ phosphorescence accompanied by weak $S_1(n, \pi^*)$ delayed fluorescence in the vapor phase. It is inferred from the temperature dependence of the emission intensity that the lowest excited triplet state of chromone vapors is $^3(n, \pi^*)$ in nature. The origins of the $S_2(\pi, \pi^*)$, $S_1(n, \pi^*)$ and $T_1(n, \pi^*)$ states were determined. The assignments of the vibronic bands in the phosphorescence spectrum were carried out based on the results of the DFT calculations at the B3LYP/6-311 + G(p, d) level. The relaxation processes in the vapor phase are discussed based on the pressure and excitation energy dependence of the relative phosphorescence yield.

References

[1] M. Sakamoto, M. Kanehiro, T. Mino, T. Fujita, Chem. Commun. (2009) 2379–2380.
[2] K. Ohara, D.M. Martino, H. van Willigen, J. Photochem. Photobiol. A 181 (2006) 325–332.
[3] S.C. Gupta, R.C. Kamboj, J. Ind. Chem. Soc. 80 (2003) 1007–1014.
[4] Y. Sakaguchi, M. Igarashi, H. Hayasi, Z. Phys. Chem. 182 (1993) 77–87.
[5] M. Igarashi, Y. Sakaguchi, H. Hayashi, Y.J. Ihaya, Chem. Phys. Lett. 181 (1991) 187–192.
[6] H. Bouanani, J. Gayoso, Compt. Rend. Acad. Sci., Ser. C 276 (1973) 399–402.
[7] J.W. Hanifin, E. Cohen, J. Am. Chem. Soc. 91 (1969) 4494–4499.
[8] J.B. Gallivan, J.S. Brinen, Chem. Phys. Lett. 10 (1971) 455–459.
[9] Y. Yamada, S. Yamauchi, N. Hirota, Bull. Chem. Soc. Jpn. 55 (1982) 2046–2050.
[10] G.A. Val'kova, T.V. Sakhno, D.N. Shigorin, A.M. Andrievskii, A.N. Poplavskii, 55, Zh. Fiz. Khim. (1981) 803–805.
[11] J.B. Gallivan, Can. J. Chem. 50 (1972) 3601–3606.
[12] J.B. Gallivan, Can. J. Chem. 48 (1970) 3928–3936.
[13] T. Itoh, Spectrochim. Acta A 59 (2003) 61–68.
[14] T. Itoh, J. Fluores. 16 (2006) 739–742.
[15] M.J. Frisch, G.W. Trucks, H.B. Schlegel, G.E. Scuseria, M.A. Robb, J.R. Cheeseman, J.A. Montgomery, Jr., T. Vreven, K.N. Kudin, J.C. Burant, J.M. Millam, S.S. Iyengar, J. Tomasi, V. Barone, B. Mennucci, M. Cossi, G. Scalmani, N. Rega, G.A. Petersson, H. Nakatsuji, M. Hada, M. Ehara, K. Toyota, R. Fukuda, J. Hasegawa, M. Ishida, T. Nakajima, Y. Honda, O. Kitao, H. Nakai, M. Klene, X. Li, J.E. Knox, H.P. Hratchian,

J.B. Cross, C. Adamo, J. Jaramillo, R. Gomperts, R.E. Stratmann, O. Yazyev, A. J. Austin, R. Cammi, C. Pomelli, J.W. Ochterski, P.Y. Ayala, K. Morokuma, G.A. Voth, P. Salvador, J.J. Dannenberg, V.G. Zakrzewski, S. Dapprich, A.D. Daniels, M.C. Strain, O. Farkas, D.K. Malick, A.D. Rabuck, K. Raghavachari, J.B. Foresman, J.V. Ortiz, Q. Cui, A.G. Baboul, S. Clifford, J. Cioslowski, B.B. Stefanov, G. Liu, A. Liashenko, P. Piskorz, I. Komaromi, R.L. Martin, D.J. Fox, T. Keith, M.A. Al-Laham, C.Y. Peng, A. Nanayakkara, M. Challacombe, P.M.W. Gill, B. Johnson, W. Chen, M.W. Wong, C. Gonzalez, J.A. Pople, Gaussian 03, Revision B.05, Gaussian, Inc., Pittsburgh, PA, 2003.

[16] H. Yoshida, K. Takeda, J. Okamura, A. Ehara, H. Matsuura, J. Phys. Chem. A 106 (2002) 3580–3586.

[17] M. Stockburger, Z. Phys. Chem. (Frankfurt am Main) 31 (1962) 350–362.